AERODYNAMIC RESULTS FOR A NOTCHBACK RACE CAR

Ştefan Bordei[1], Florin Popescu[2]

[1]PhD student, "Dunarea de Jos" University of Galati,
[2] Professor, PhD eng, "Dunarea de Jos" University of Galati

stefanbordei@yahoo.com, florin.popescu@ugal.ro

ABSTRACT

The use of numerical simulations is nowadays drawing an increasing interest in aerodynamic shape optimization. We firstly present a thorough benchmark of different numerical experiments done with Fluent, CFX, OpenFOAM and PowerFLOW on the Ahmed body in order to select the proper model and numerical scheme for our needs. Numerical strategies for reducing preparation, discretization, simulation and time optimization are also shown. Secondly, results around a NACA airfoil are discussed. As an application we consider the air flow around a notchback race car. The results presented show that the chosen strategy is able to accurately predict drag, lift and aerodynamic efficiency with low computational cost.

KEYWORDS: Fluent, CFX, OpenFoam, PowerFLOW, numerical methods, car simulation.

1. Introduction

The synergy between computational fluid dynamics (CFD) and wind tunnel testing has increased the potential for optimization in external aerodynamic development of race cars. CFD in motor sport is often used to optimize car shapes for downforce and drag, correlations with wind tunnel tests and track tests. The best example is the CFD based development process of the DBR9 racecar [27] which started from a CFD model and went directly to the race track. It won the 24 hours Le Mans race.

In order to perform the optimization of the rear wing shape on the racecar we needed to converge towards a reliable and accurate method of simulation that would enable us to compare results for several alternative wing modifications. The approach is always subject to constraints like available RAM and total CPU time. These constraints determine the modeling strategy used in terms of total number of grid points and the complexity of numerical models. The more resolution you have the better the accuracy (except if the y+ value is wrong than results will be worst), but longer total CPU time, therefore the difficult part is to find the best compromise between the cost of the simulation and the accuracy. Why would CFD accuracy be so important? A good example would be the WINGGRID [33] a highly efficient patent for reducing induced drag by more

than 50% that, to this day, its aerodynamic efficiency has never been matched by CFD simulations quantitatively [19]. But then again there is an up to 5% error between different wind tunnels aerodynamic coefficients on the same geometry [34]. Flight tests for the blended winglet showed a 7% drag reduction while wind tunnel tests showed only a 2% reduction [14], this means that final validation should always be done in the natural environment that the wing will operate: flight tests for aerospace and track tests for motor sport.

The present paper presents a benchmark of 138 numerical simulations in order to quantify from accuracy, RAM and CPU time point of view the drag, lift and aerodynamic efficiency so we can pin point the best. We do not intend to describe in detail all of them, but to highlight the best practices from our experience. First, we compare different numerical results with results from the literature [9] on the well known Ahmed body model [1]. Furthermore, we present a detailed analysis on a car with simplified underbody and closed air inlets from [3]. The performance of the rear wing is strongly influenced by the coupling between various elements like the rear windshield angle with relation to the x-axis, the C-pillar, the length of the rear trunk lid [34].The quality of the flow towards the rear wing can be influenced even by the radius and the angle of the A-pillar [21] and by the shape and position of the mirror.

This means that studying the wing alone is not sufficiently relevant, due to the impossibility of replicating the complex interactions between the various car elements through the usage of simple boundary conditions. Also, the rear wing induces an increase of the negative pressure coefficient magnitude along the whole underbody of the racecar which creates more downforce than the wing alone would be able to produce [14].

The paper flows as follows. Section 2 contains the Fluent, CFX, OpenFOAM and PowerFLOW descriptions. Section 3 contains the solving recommendations. The results and numerical examples for the Ahmed body, the NACA airfoil and the simplified car are presented in Section 4. The conclusions are drawn in Section 5.

2. Simulation software description

In the present embodiment the effort is aimed at answering the following question: which solver formulation, from an accuracy point of view, is the best today?

Fluent, CFX, PowerFLOW and OpenFOAM have been investigated and compared with findings in the literature for PowerFLOW [5], OpenFOAM [31], [17], [19] and Star-CCM+ [23] .

The answer is Star-CCM+ with a 0.018% drag error [23], accuracy wise, which is the most important criteria for us. The T-SST (Fluent) model manages to get the best results for minimum Cl error and minimum aerodynamic efficiency (k) error.

2.1 Fluent description

The new version of ANSYS Fluent [2] incorporates features like the scale adapted simulation (SAS) turbulence model and automatic shape flow optimization for fluid dynamics analysis using gradient information, mesh-morphing technology and an optimizer. This is at a time when PowerFLOW does not, yet, integrate an imbedded optimizer, but the morphing comes after ANSA's implementation.

The Fluent simulation strategy is illustrated in Fig. 9.

The steady and transient solvers were both used.
Linear solver: V-Cycle (AMG) for all.
Pressure-velocity coupling: SIMPLEC
Discretization Scheme: Second Order for pressure and Second Order Upwind for the rest. Relaxation Factor: 0.65 for Pressure and 0.5 for the rest.

Turbulence models used: Spalart-Allmaras, realizable k-ε (RKE), k-ω Shear Stress Transport (k-ω SST), Transition k-kl-w, Transition -SST, Reynolds Stress Model (RSM), Large Eddy Simulation (LES), Detached Eddy Simulation (DES), scale adapted simulation (SAS) and v2f.

Wall functions: standard wall functions.

2.2 CFX description

CFX with its adaptive wall functions makes the best use of available mesh resolution this is the reason why its number 1 for average ΔCd and 3rd for ΔCl, it loses points as it is only 6th place for aerodynamic efficiency Δk=Cl/Cd. Its interpolator is seen as a serious advantage over PowerFLOW's coarse-to-fine method and OpenFOAM's interpolator, as it facilitates optimization of shapes while reducing simulation time, not to mention its readiness for 2 way aero-structural coupling throw the ANSYS workbench [3].

The steady and transient solvers were both used.

For the transient simulation we used a time step adaptation: maximum timestep 0.0005 [s] and minimum timestep 5e-05 [s].

Solver control:

Turbulence numerics and advection scheme: high resolution.

- Body forces:
  - Body force averaging type: volume-weighted.
- Convergence control:
  - Maximum number of coefficient loops: 10 and minimum: 1.
- Convergence criteria:
  - Residual target: 0.000001
  - Residual type: RMS
- Transient scheme:
  - Second order backward Euler
- Velocity pressure coupling:
  - Rhie Chow option: fourth order
- Turbulence model used: k-ω SST
- Turbulent wall function: automatic.

2.3 PowerFLOW description

This three dimensional code is based on Lattice Boltzmann method (LBM) a recent and versatile tool for developing numerical schemes for simulating fluid flows in complex geometries.

Lattice Boltzmann method is playing a dominant role in the computational fluid dynamics community [30]. These discrete-velocity models are based on a special discretization of macroscopic kinetic equations, i.e., by constructing simple kinetic models, incorporating the essential physics of microscopic processes and applying novel numerical discretizations on these kinetic formulations. Clearly, the discrete-velocity models are based on the Boltzmann equation and kinetic theory rather than Navier-Stokes equation and continuum theory. In addition to theoretical generality, kinetic methods may have computational and numerical advantages, because the Boltzmann equation is a first-order linear partial differential equation (PDE) as opposed to Navier-Stokes equation, a second-order nonlinear PDE.

Turbulence models used: RNG k-ε (the only one available)

Wall functions: the so called 'law of the wall' (the default and only one available).

According to our results PowerFLOW (PWF) has the best boundary condition transparency at iso-distances from the Ahmed body when compared with Fluent, CFX and OpenFoam. The PowerFLOW DISCRETIZER achieved the lowest number of volume cells at iso-grid strategy (15.8 M less cells than HARPOON). From a qualitative point of view it gets the flow topology right.

We ruled out PowerFLOW with the D3Q19 Lattice Boltzmann Method and RNG k-ε model because of its current temporary issues with accuracy: 59% relative drag error (14th in Fig. 11) and 6.5% lift error (9th in Fig. 12). The temporary fix for this issue is similar to the principle presented in reference [25], except that the flow regime is not supersonic for road vehicles and the sensing function is different. However we still appreciate PowerFLOW for being the only commercially available Lattice Boltzmann Method, so it scores high for innovation and theoretical advantages over the RANS approach [5], [7], [11], [17], [12], [12], [36].

2.4 OpenFOAM description

OpenFOAM is very appealing from an economic, research [31],[17] and development [19] stand point. It is in stark contrast to PowerFLOW's high price. OpenFOAM has faster convergence then Fluent but is less accurate at iso-resolution. For example the drag coefficient error: 15.2% for k-ω SST OpenFoam compared to 6.8% for S-A Fluent and 4.6% for Fluent k-ω SST while using the same 1.6M grid. OpenFOAM loses points because of (the lack of) user-friendliness and documentation for more advanced features[25] like automated optimization already feasible in OpenFoam 2.0.0. [25].

The flow solver used: SimpleFoam, steady state. As far as schemes for discretization go the fallowing were used:

Grad Schemes: Gauss linear.
Div Schemes: Gauss upwind.
Laplacian Schemes: Gauss linear corrected.

The linear solver was: GAMG (Multigrid) with smoother: Gauss Seidel and *nCellsInCoarsestLevel* 150 also the solver tolerance was 1e-7.

The relaxation factors were 0.3 for pressure and 0.7 for the other variables (U, k and omega). The turbulence model used was: k-ω SST with the: *omegaWallFunction*.

3. Solving recomandations

3.1 Boundary Conditions

It is crucially important to replicate, through appropriate boundary conditions, as much as possible the experiment to which you wish to compare the results [26]. A good simulation can be made invalid by a simple part that was not up to date (this, of course, is true for wind tunnel tests also).

The recommendations for Fluent boundary conditions go as follows.

Set up:

- Velocity inlet boundary condition with a Fig. 4 type profile that would gradually increase the velocity until final simulation velocity is reached. We must emphasize that this was proved to reduce the total number of iterations up to 65%! The first comparison was made between the iterations required to converge the residuals and the drag coefficient, Cd, of two transient cases on the same geometry with different resolutions. The first 6 million case took 87 300 iterations to converge with an S-A model and normal initialization with the final inlet velocity [21] and the second 15 million case took 30 000 iterations with a RSM model but we used the Fig. 4 type initialization. If we further compare other simulations done with the S-A model, on the same geometry, but similar resolution, than the gain is even higher: up to 76%. If, again, we further compare with a hexahedral dominant grid than the gain is 84%. The reason for which the initialization using a velocity value equal to 0.024*final (determined by trial and error) desired inlet velocity reduces computational effort is that this method provides the flow with a smooth transition to the desired inlet velocity and it avoids higher initial Cd values that would appear when initializing with zero velocity or the final inlet velocity. As this first low speed ($V_\infty \neq 0$ m/s) case advances and iterates, it resolves the flow (for residuals 1e-3) and as the velocity is increased it serves as a good "guess" for the slightly higher speed. Another advantage is that the Cd value for the first iteration is better scaled, closer to the final one then an initialization with the final inlet velocity from the beginning which helps considerably with the total number of iterations. This finding enabled us to carry out more high fidelity simulations in less time. It was noted that this approach does not work with PowerFLOW.

- Boundary layer suction, this is where the shear stresses will be set to zero in the simulation, all modern state of the art wind tunnels have this feature. This is important because we want to get the same road boundary layer height in the simulation as the wind tunnel we are comparing results to;

- The dynamic mode: rotating wheels and moving ground (belt) can be replicated in ANSYS FLUENT via the Rotating Wall Boundary Condition for the tires, moving frame of reference (or moving mesh → more expensive but not actually more accurate!) for the spokes and Moving Wall Boundary Condition for the belt [2]. Without the moving ground Boundary Condition (BC) the level of downforce of the vehicle will no doubt be false, making the impact of the rear wing on the vehicle total downforce impossible to evaluate in comparison with track tests;

- The exit of the virtual wind tunnel should be set up as Pressure Outlet Boundary Condition;

- Radiators, intercoolers, condensers and other heat exchangers can be set up as porous media fluid;

- The rest of the domain boundaries can be set up as Symmetry Boundary Condition.

3.2 Turbulence Modeling and Transient Simulation

Based on our experience, the most appropriate turbulence model from a quantitative stand point, for motor sport external aerodynamics is the Fluent RKE model. For the qualitative criteria the k-ω SST Fluent turbulence model gave the best correlation with experiment. With an optimum grid, it is the best turbulence model for capturing the separation lines, the strong vortices and wake physical structure with low computational resources and good accuracy. From a resources point of view the Spalart-Allmaras turbulence model is most suited for an automated aerodynamic optimization task if the objective function is focused on drag minimization and if time is taken to find the grid optimum for the S-A.

Begin the simulation with the RKE Fluent model (see Fig. 9).

Recommended settings for the RKE:

- Start with a steady solver

- Initialize the flow field with a value of 0.024*final inlet Velocity (Fig. 4). Then gradually increase the velocity by one meter per second every fifty iterations until you reach your desired simulation inlet velocity.

- Set Under Relaxation Factors for the RKE to:
  o   0.65 for Pressure,
  o   0.35 for Momentum and
  o   0.50 for k and epsilon.

- We recommend the first 50 iterations with First Order Discretization then switch to Second Order, and increase the velocity by 1 m/s (Fig.4);

- If convergence problems occur right at the beginning of the simulation, set Under Relaxation Factors for k and epsilon to 0.2 for 50 iterations, and then switch to 0.5 and after that switch to Second Order Discretization [21].

- An algebraic multi-grid (AMG) method is recommended, to accelerate solution convergence. Solver Type: V cycle for all (pressure, momentum, modified turbulent viscosity etc), stabilization method: RPM if you have InfiniBand if not use "flexible" instead;

- The SIMPLEC algorithm, is advised for the pressure – velocity coupling.

- After the convergence of the residuals (1e-6) and Cd (±1e-3) value, check that the average y+ value is between 30 and 300 (if the average y+ value is out of the desired range redo the grid with a different grid strategy: if the y+ is too high refine else coarsen).

- Switch to the transient solver.

- Continue with the RKE.

- At the beginning of the transient calculation, start with a time step of 5e-5.

- If the residuals or the Cd do not converge set the time step to 1e-6 and the AMG from the V-cycle to the W-cycle (if you have InfiniBand).

- We let the flow particle pass the length of the vehicle 5 times and that usually results in converged drag values, but for some road vehicle shapes and turbulence models it takes 12 times to see converged values.

- If still convergence issues then double the resolution (1/2*base level) or reduce the time step even further (1e-07).

4. Results and numerical examples

4.1 Ahmed Body
4.1.1 Geometrical description

The Ahmed body is a well known reference body for road vehicles flows [1]. The geometrical description is presented in Fig.1. In the present embodiment we studied the 25o and 12.5o slant angles (φ).

4.1.2 Boundary conditions

The inlet of the domain is defined in Fluent as velocity-inlet, in CFX as inlet (subsonic), in OpenFoam as inlet, in PowerFLOW as inlet velocity. The Ahmed body and the road are set as wall, no slip boundary condition in all the applications used here. The side walls and sealing are set as symmetry in Fluent, as free slip wall in CFX, as frictionless wall in PowerFLOW and in OpenFoam as slip. The outlet of the domain is set as pressure-outlet in Fluent, as outlet (subsonic) in CFX, as inletOutlet in OpenFOAM and as outlet: static pressure, free flow direction in PowerFLOW. The visual equivalent of the fore mentioned description is presented in Fig.5 and Table 3.

The best inlet boundary condition transparency was observed for PowerFLOW.

Turbulence models used: Spalart-Allmaras, realizable k-ε (RKE), RNG k-ε (in PowerFLOW), k-ω Shear Stress Transport, Transition k-kl-w, Transition Shear Stress Transport (T-SST), Reynolds Stress Model (RSM), Large Eddy Simulation (LES), Detached Eddy Simulation (DES), scale adapted simulation (SAS) and k-ε-v2 (or v2f).

4.1.3 Meshing

Complex geometry cleaning and meshing are the most repetitive and time consuming processes in automotive CFD today [16].

HARPOON or SPIDER, are recommended for the automated volume to surface grid generation because we obtained some of our best results with hexahedral grids. These meshes are easily transformed in polyhedral grids that gave even more accurate results. HARPOON creates the fastest unstructured, hexahedral dominant grid when compared to the rest. There is no need for cleaning of the geometry and the software is user friendly. You pass from days and weeks for the preparation of the

model to hours and minutes because it has the fastest meshing algorithm on the market.

The grid strategy proposed here can be applied with other meshing software like ANSA, snappyHexmesh or SPIDER.

The simulation domain can be effortlessly created by simply making use of the far-field option in HARPOON [31]. The recommended reference surface length is 5 mm on the car [21]. This surface reference length recommendation is also based on the best results for drag on the Ahmed body (see Fig.11).

The simulations on the Ahmed body geometry [1], [9] were done for 13 different grid resolutions: 200k, 500k, 530k, 1.3M (500k transformed in polyhedra), 1.68M, 1.79M (polyhedra), 1.9M, 5M (1.9M transformed in polyhedra), 7.69M, 13.8M, 14.58M, 14.6M and 23.5M elements see Table 4 for more details.

The base level (far field) for the coarse 500k grid (see Fig. 8a) is 160 mm, reference surface length is 5 mm with 2.5 mm in areas of separation and the finest refinement zone was a 10 mm grid cell size. Refinement zones are what HARPOON uses for controlling the resolution of the cells in the volume. The domain size, for the half model is X [-10m; +25m], Y [0; +4m], Z [0; 10m] with the origin on the ground at the rear (Cb from [1]) of the Ahmed body. The speed of the meshing software can be measured in term of cells per minute. For HARPOON the cells per minute = 2 738 128 and is seen as the fastest for today's market.

The base level for the medium 1.9M grid (see Fig. 8b) is 160 mm, reference surface length is 1.25 mm and the finest refinement zone was a 10mm grid cell size.

The domain size is the same as the coarse grid. Cells per minute (HARPOON) =4 829 891.

The base level for the fine 13.8M grid (fig 8c) is 80 mm; the surface mesh length varies according to the pressure coefficient in the range: 5mm to 0.625mm. The simulation domain is drastically reduced to test the transparency of the boundary conditions: X [-10.44m, 22m], Y [±0.93m], Z [0, 1.4m]. Cells per minute (HARPOON) =5 745 942. This is at least twice as fast as the PowerFLOW DISCRETIZER or than SPIDER, ANSYS Mesher, CFX Pre, Gambit, T-Grid and ANSA.

The base level for the fine 14.58M grid (Fig. 8d) is 80 mm, the surface reference length is 1.25mm and the finest refinement zone was a 2.5mm grid cell size. The domain size is X [-2.13m; +10m] Y [-1.5m; +1.5m] Z [0; 3m] with the origin same as reference [1], i.e. at the middle of the model on the ground. Cells per minute = 4 071 070.

The boundary layer on the Ahmed body is done after the whole domain is discretized, settings for the boundary layer: initial cell height: 0.2 mm, number of layers: two (attempts with 5 and 10 failed with version 4.1 but fixed in 4.2) and constant expansion rate of 1.2.

The findings for the successful grid strategy for the full scale car agree also with reference [37] for the wake resolution for example.

The amount of drag experienced by a full size road vehicle is strongly related to the structure of the flow in its wake up to as much as Cd*A=0.110 m2 for an unbalanced wake.

The wake topology simulation results were compared with reference[9]; see Fig. 7, for a slant angle of 25o. Analysis of Fig. 7 and of the relative error, leads to a hierarchy between the different methods.

The two grids for PowerFLOW were thought as follows: the 530 K grid uses the same strategy as Fig.8a but because the PowerFLOW DISCRETIZER churns out fewer cells at iso-grid strategy we added 2 cells in the boundary layer (see Table.4) to get closer to the cell count in Fig.8a. The second grid was done according to the grid optimum found by EXA's own Ehab Fares [5].

4.1.4 Results

From a qualitative stand point the k-ω SST 13.8M case is the best as shown in Fig.6b (if not explicitly specified simulations are transient). The SAS is the best when it comes to grid independency (see Fig. 14.) as indicated by the average ΔCd.

The smallest relative error, quantitatively, for the drag coefficient is achieved by the S-A (0.53% in Fig.11) then by the SST-CFX (steady) followed by RKE (steady) with the T-SST being 9th place. The smallest relative error for lift coefficient is achieved by T-SST (0.27%) followed by k-ω SST (OpenFoam) and v2f (see Fig.12). The smallest relative error for aerodynamic efficiency is obtained with T-SST (2.82%) followed by RKE (steady) and SAS (see Fig.13). When comparing the results for the Cd of the 12.50 case, the first is the LES (0.73%) followed by RSM, RKE and DES (see Fig.17).

The Spalart-Allmaras turbulence model is good for predicting the aerodynamic performance of the wing (see the results in section 4.2.4) in a wide operating range. With the correct resolution it can even accurately predict the quantitative drag of the Ahmed body better than the k-ε two equation model and the three equation model (k-kl-w) or the seven one (RSM). This means that is the least expensive (computationally) and most suited for automated aerodynamic Cd optimization cases if time is taken to find the grid optimum. It comes at 1st place (0.53%) for minimum drag (the 500k hexahedra grid transformed in 1.3M polyhedra in Fig.11), 5th for minimum lift (13.8M grid in Fig.12) and 7th for aerodynamic efficiency k (1.9M in Fig.13). It is 5th for both average ΔCd (Fig.14) and average ΔCl (Fig.15) while for average Δk its place is at number 9 (Fig.16). The indicator for simultaneous drag, lift and aerodynamic efficiency quantitative prediction was chosen as R=SQRT (ΔCd2+ΔCl2+Δk2). For this criteria S-A is at number 11 (see Fig. 18). This clearly shows the need for grid optimization for the S-A to

work properly. S-A is still a relatively new turbulence model [5] with potential for improvement and perhaps in a future version it will outperform the RKE for lift predictions also.

The Realizable k-epsilon model predicts quite well the drag coefficient value, and is robust. It gave the second best consistent results for drag, lift and aerodynamic efficiency (see Fig.18) simultaneous prediction. We can see why it is chosen as the work horse for industrial external aerodynamics simulations. We should keep in mind that it comes at less of a computational cost than the RSM, LES and DES. It is 3rd in the 12.5o 14 M case (Fig.17) and 3rd in the 25o 500k case as far as drag is concerned (see Fig.11). For lift and aerodynamic efficiency it reaches 4th place (Fig.12) and 2nd place (Fig.13) respectively. For Cd and Cl grid independency it ranks 3rd place and 2nd place respectively (Fig.14 and Fig.15). In the Star-CCM+ formulation it achieves a 0.018% drag error [23] for a wind tunnel reference car model, claming 1st place when correlated with all of our results.

The k-ω SST (13.8M) Fluent model achieved the best correlation in terms of qualitative wake comparison with experiment (Fig. 6b and Fig. 7a). It comes at 2nd place for minimum drag in the CFX formulation (1.9M case in Fig.11) and 2nd place for lift in the OpenFoam formulation (Fig.12); 5th place for aerodynamic efficiency in the Fluent implementation. The SST from CFX had the fastest converging time from them all except for S-A. The k-ω SST formulation in OpenFOAM would gain 2st place for the Ahmed body ΔCd (0.33%), 9th place for ΔCl (8.4%) and 10th place for Δk (8.71%) according to the results in [31]. Also we know from the aerospace literature that the CFX formulation is among the best for complex wing configurations [22].

The T-SST turbulence model is 1st for lift (Fig.12) and for aerodynamic efficiency (Fig.13) in our top 14, but only 9th place for drag (Fig.11) and it ranks 1st place as far as grid independency is concerned for lift (see Fig.15). It manages to achieve 5th place for average Δk (Fig.16). When combined with the S-A it alleviates some of the drag error but it degrades the lift prediction also, although it still surpasses the RKE for lift an aerodynamic efficiency with a penalty in the total number of iterations (see Table 1).

The v2f turbulence model is at number 6 for drag (7.7%), number 3 for lift (1.3%) and 12 for aerodynamic efficiency (9.6%). In reference [37] the k-ε-v2 (or v2f) achieved a ΔCd=1.5% which would place the v2f model at number 4 in our top 14 if we were to consider the 35o slant just as hard to numerically model as the 25o slant angle.

As mentioned in reference [21], with the same fine resolution, the RSM Fluent model gives more accurate (0.3% for drag) results than the realizable k-ε (2.1%) for realistic road vehicles shapes on the same geometry. We found the same correlation for the 14M

grid (12.5o) and for the 1.9 M (25o) case which means that for a equilibrated wake RSM outperforms RKE and also for a unbalanced wake as long as the resolution is kept high enough for RSM to work.

The Large Eddy Simulation (LES) proved that when it comes to Cd values, with an optimum grid it can be number 1 for the 12.50 slant angle (see Fig.17) at least (the value in table 2 is an average on the last stabilized frames). For the 25 slant angle we did not find the grid optimum for the LES.

The Very Large Eddy Simulation (VLES) with the RNG k-ε turbulence model within PowerFLOW achieved very poor correlation for quantitative drag and aerodynamic efficiency (last place in Fig11.) and 9th place for quantitative lift but good correlation for qualitative averaged results (not shown here). Even if the optimum grid strategy from [5] and the best practices from [7] were applied.

The Detached Eddy Simulation (DES) Fluent turbulence model is placed at number 13 in the drag and lift prediction hierarchy (Fig.11 and Fig.12), and 4th for aerodynamic efficiency (Fig.13) for the 25o slant angle. As for the 12.5o slant the DES with k-ω SST ranks 4th with a 4.6% drag error and 5th for DES with RKE as the underlying RANS (Fig.17). Overall the DES for simultaneous drag, lift and aerodynamic efficiency quantitative prediction takes 10th place. If the topology of the flow is checked than it is noticed that instantaneous results for DES look like the averaged, stabilized VLES results [7], [9]. We observe a better match with experiment for DES.

The Scale Adapted Simulation (SAS) is the first in Fig.18 for simultaneous drag, lift and aerodynamic efficiency quantitative prediction. As far as drag is concerned it comes at number 5 with a 2.5% error (Fig11). For lift the SAS is placed at number 10 (Fig.12) and for aerodynamic efficiency at no. 3 (Fig.13). The qualitative results for SAS are far from the experimental results.

4.2 N.A.C.A 4412 Airfoil

The benchmark for the airfoil was deemed necessary in order to properly model the rear wing on the road vehicle.

4.2.1 Geometrical description

The well known N.A.C.A 4412 airfoil from reference [28] with 4% camber at 40% chord and 12% thickness is presented in the inset in Fig.6a.

4.2.2 Boundary conditions

The Fluent boundary condition for the inlet (the semicircle and top and lower horizontal edges in Fig.6a) is velocity-inlet, the airfoil is set as wall, no slip and the exit is pressure-outlet.

4.2.3 Meshing

The structured 12195 quadrilateral cells mesh is done with GAMBIT and is shown in the inset in Fig.6a. The first cell height is 1.655mm with the y+ varying between 33 (for RSM at α=22.1o) and 294 (for RKE at α=22.1o) depending on the turbulence model and angle of attack.

4.2.4 Results

For the calculation of airfoil lift in free air the best method is actually the panel method with the Baldwin-Lomax algebraic turbulence model (see Fig.6a) the 3rd smallest absolute lift error is the RSM model for angles of attack α<100 but the Transition Shear Stress Transport (T-SST) turbulence model has the smallest CFD error (2nd) not only for the high alpha range (like the S-A), but for the entire range of angle of attack. All the simulations had the same structured quad grid (top, center in Fig.6a). They were all compared to the wind tunnel test in reference [28]. From this comparison the best practice for CFD is: the T-SST model. The panel method Visual Foil used in Fig.6a is that of Dr. Patrick E. Hanley. This is the method used to find the airfoil in the patent application A/00551.

4.3 Notchback race car
4.3.1 Geometrical description

The simplified car from [3] was used as an accessory to the rear wing in order to match the operating environment that it will face. The geometrical description of the vehicle can be seen in Fig. 2. The simulation volume is 52 meters long, 3 meters high and wide with the wheelbase center at 12,222 m from the inlet. In terms of the influence of the car on the rear wing airfoil and height, the angle of the rear windshield with relation to the x-axis (25.8^o on this particular car), the C-pillar (Radius =907mm) and the length of the rear trunk lid are of first order. The radius of the A-pillar (Radius =41 mm) and the mirror are of second order. A ruled based optimization would dictate an A-pillar radius of 100 mm and the angle of the rear windshield =$11^o \div 15^o$.

4.3.2 Boundary conditions

The inlet of the domain is set as velocity-inlet, the side wall, sealing and the symmetry wall as symmetry. The outlet as pressure-outlet, the car and the road as set up as wall, no slip. The Detached Eddy Simulation was chosen as the turbulence model.

4.3.3 Meshing

Three discretizations were made to asses the grid convergence. These were 1.8M, 3.57M and 5.85M. The reason the last grid is not 7.3 M is that the simulations for this case, were done on a low resources machine and more than 6 M would have occupied the entire available RAM. However we still managed to reach grid convergence as shown in Fig. 10.

4.3.4 Results

The results on the simplified car geometry from [3] with a rear wing are summarized in Fig.3 and Fig.10. The drag coefficient 0.438 seems a bit excessive for this type of road vehicle shape (notchback). But than again we know from the Ahmed body results that the DES can have between -21% to +33.6% quantitative errors. In this instance is obviously around +33% which would place the correct Cd value to 0.291. Even tough the angle for

the rear window is 25.8^o the flow remains attached. This is not some fluke of the numerical method, this can also be seen in wind-tunnel tests if the radius of the C-pillar is >900 mm. The separation bubble seen on the Ahmed body with φ=25° both in the wind – tunnel test [9] and our simulations (Fluent kω-SST or PowerFLOW) can be eliminated if the radius for the C-Pillar is optimized, while keeping the same slant angle. In this way the normal road vehicle gets to have good ergonomics, beautiful design and good aerodynamics all at once. However if the road vehicle is a race car than, constrains for beautiful design and ergonomics are minimized and the slant angle optimum converges to 11°. This impacts the height of the rear wing relative to the car: higher for slant >25 ^{o} and lower when slant <12 ^{o}. The local angle of attack of the rear wing is piloted by the slant angle. For the simplified car from [3] it is 26°, this trend will be also confirmed for the modified F40 in future work.

5. Conclusions

In this paper, we have presented a comprehensive study for realistically predicting airflows around cars. The focus is on high fidelity road vehicle simulations, but with as short as possible turnaround time as prerequisite for aerodynamic optimization and innovation at lower development cost. The airflow is modeled using different commercial CFD packages, i.e. Ansys Fluent, CFX, OpenFOAM and PowerFLOW. Furthermore, recommendations for geometry preparation, grid and case set-up are given.

Results for a road vehicle indicate that the best solver from an accuracy point of view is Star-CCM+ [23].

For Fluent the Spalart-Allmaras model was found to be the most accurate in term of drag and this is considered as a new finding as far as automotive CFD is concerned since most researchers consider other turbulence models more accurate for the Ahmed body.

The Fluent formulation of Transition Shear Stress Transport turbulence model was discovered as the best candidate for aerodynamic efficiency and lift prediction for the Ahmed body; this is also considered as a new finding.

It was noted that a decrease of the total number of iterations of up 84% can be achieved if our scheme for smooth velocity initialization is used (for a hexahedral dominant grid). PowerFLOW has been found to have the best inlet boundary condition transparency. Best quality to cost ratio belongs to OpenFOAM.

Finally we would like to point out that HARPOON is the fastest meshing software when compared to the ANSA, PowerFLOW DISCRETIZER, ANSYS Mesher, CFX Pre, Gambit and T-Grid. Our best results where achieved with a HARPOON grid, but for very complex geometries

ANSA was the most reliable. The polyhedral grid gave consistently better results than the hexahedral grid when transformed in Fluent from both ANSA and HARPOON original meshes.

The presented results for the notchback race car agree well with the expected ones.

In a forthcoming paper, we will focus on multidisciplinary system design optimization for the rear wing but with a complex underbody for a FIA GT I race car built from scratch (7 milestones) inspired by the Ferrari F40 with a newly developed aerodynamic kit. The new rear wing will try to beat the state of the art for 2 targets. One is for maximum aerodynamic efficiency at 3 Reynolds numbers and the second is for maximum absolute lift coefficient. The state of the art is represented by some of the best aerospace high lift airfoils and by motor sport developed rear wings such as APR Performance, the US 20040256885 patent, Simon Mc Beth's ReVerie Exige, the DE10047012 Porsche patent, the 2010 Lamborghini Sesto Elemento concept and Bugatti Veyron.

ACKNOWLEDGEMENTS

REFERENCES

[1] **Ahmed, S.R., Ramm G.**, 1984, *Some Salient Features of the Time-Averaged Ground Vehicle Wake*. SAE Technical Paper 840300.
[2] **ANSYS FLUENT 13.0**, 2011. *User Guide and Tutorial Guide*.
[3] **ANSYS CFX 13.0,**. 2011. *User Guide and Tutorial Guide*.
[4] **ANSA 13**, 2009. *User Guide and Tutorial Guide*.
[5] **David C. Wilcox**, 1994. *Turbulence Modelling for CFD*.
[6] **Ehab Fares**, 2006. *Unsteady flow simulation of the Ahmed reference body using a lattice Boltzmann approach*.
[7] **Exa Corporation**, 2006. *PowerFLOW Best Practices Comprehensive Guide of: Geometry Preparation, External Aerodynamics, Aeroacoustics, and Thermal Management*.
[8] **Exa Corporation**, 2006. *PowerFLOW User's Guide*.
[9] **Exa Corporation**, 2006. *PowerViz User's guide*.
[10] **H. Lienhart, C. Stoots, S. Becker**, 2009. *Flow and Turbulence Structures in the Wake of a Simplified Car Model (Ahmed Model)*.
[11] **HUDONG CHEN et al**. 1997. *Digital Physics Approach to Computational Fluid Dynamics: Some Basic Theoretical Features*.
[12] **HUDONG CHEN et al.**, 1998. *Realization of fluid boundary conditions via discrete Boltzmann dynamics*
[13] **HUDONG CHEN,** 1998. *Volumetric formulation of the lattice–Boltzmann method for fluid dynamics: Basic concept*.
[14] **Joe Clark**, 1999. *Personal communication*.
[15] **Joseph Katz**, 2006. *Race Car Aerodynamics Designing for Speed*, 246-247.
[16] **Kent P. Misegades et al**. *Rapid Mesh Generation for Fluent Automotive Simulations*.
[17] **Louis Gagnon, Marc J. Richard**, 2010. *Parallel CFD of a prototype car with OpenFOAM*
[18] **Mehtab Pervaiz and Christopher Teixeira**, 1999. *Two Equation Turbulence Modeling with the Lattice-Boltzmann Method*.
[19] **M. Islam, et al.**, 2009**.** *Application of Detached-Eddy Simulation for Automotive Aerodynamics Development*.
[20] **M. J. Smith et al.**, 2001. *Performance Analysis of a Wing with Multiple Winglets*. AIAA-2001-2407.
[21] **M. Lanfrit**, 2005. *Best Practice Guidelines for Handling Automotive External Aerodynamics with FLUENT*, Version 1.2
[22] **Murand et al.**, 2004. *Simulation of Vehicle A-Pillar Aerodynamics using Various Turbulence Models*. SAE Technical Paper 2004-01-0231
[23] **Nicolas Thouault et al.**, 2009. *Numerical analysis of design parameters for a generic fan-in-wing configuration*
[24] **Nor Elyana Ahmad et al.**, 2010. *Mesh Optimization for Ground vehicles Aerodynamics*, CFD Letters, 54-65.
[25] **OpenFoam User Guide** v2.0.0, 2011
[26] **Rainald Löhner**, 2008, *Applied Computational Fluid Dynamics Techniques: An Introduction Based on Finite Element Methods*, Second edition, pp. 167-169
[27] **Rob Lowis & Philip Postle**, 2003, *CFD Validation for External Aerodynamics*
[28] **Rob Lowis**, 2006. *Aston Martin beats the 24 hour clock*.
[29] **Robert M Pinkerton**, 1937, Report No. 563 *Calculated and Measured Pressure Distributions over the Midspan Section of the N.A.C.A 4412 Airfoil*.
[30] **S.Chen, G.D. Doolen**, *"Lattice Boltzmann methods for fluid flows"*, Ann. Rev. Fluid Mech. 30, pp. 329-364, 1998.
[31] **Sebastian MÖLLER, et al.**, 2008, *Investigation of the flow around the Ahmed body using RANS and URANS with various turbulence models*.
[32] **Shark Ltd**, 2011. *Harpoon User Guide*.
[33] **Ulirch La Roche** US Patent 5823480, 1998. *Wing with a Wing Grid as the End Section*.
[34] **W.H. Hucho**, 1998, *Aerodynamics of Road Vehicles*, 4th Edition, SAE International.
[35] **W. Meile**, 2007. *Forces and pressure distribution*.
[36] **Yangbing LI et al.**, 2004. *Numerical study of flow past an impulsively started cylinder by the lattice-Boltzmann method*.
[37] **Yunlong Liu, Alfred Moser**, 2003. *Numerical modeling of airflow over the Ahmed body*.
[38] **Zenitha Chroneer**, 2007. *The CFD Process for Aerodynamics at Volvo Cars using HARPOON-FLUENT*.
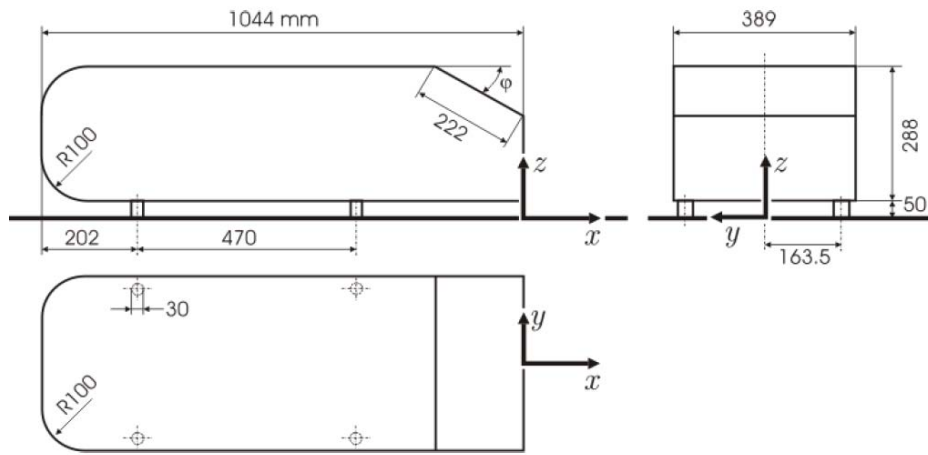
Annexes

Fig. 1. *Geometry of the Ahmed reference model (dimensions given in mm)*

Table 1. *Simulation results for the Ahmed Body with 25° slant angle*

Mesh size and turbulence model	Ahmed Body Slant 25°					
	Cl	Cd	k	Iterations	Ds [mm]	Avg y+
Experiment [34]	0.345	0.299	1.154	-	-	-
500k RKE steady	0.339	0.302	1.125	2,587	0.200	248.5
500k RKE Unsteady	0.331	0.304	1.088	9,669	0.200	248.0
1.3M Polyhedra RKE steady	0.305	0.295	1.036	2,644	1.533	193.2
1.9M RKE Unsteady	0.357	0.374	0.956	11,139	0.869	112.0
13.8M RKE unsteady	0.364	0.349	1.042	86,974	2.113	14.0
23.5M Hexa RKE unsteady	0.385	0.312	1.234	31,165	0.716	90.42
500 k RSM	0.437	0.410	1.066	2,150	0.200	248.0
1.9M RSM	0.332	0.259	1.281	7,323	0.869	104.0
500 k DES	0.305	0.234	1.306	4,451	0.200	206.0
1.9M DES	0.474	0.399	1.186	12,000	0.869	112.0
500 k LES	0.377	0.356	1.058	3,500	0.200	229.0
1.9M LES	0.302	0.241	1.254	24,326	0.869	92.0
13.8M LES	0.234	0.427	0.547	28,600	2.113	10.2
500 k T-SST	0.300	0.267	1.126	8,542	0.200	224.6
1.9M T-SST	0.344	0.260	1.323	19,600	0.869	206.4
5M T-SST Polyhedra	0.347	0.255	1.362	40,447	0.736	86.8
1.9 M T-SST+S-A Polyhedra	0.311	0.288	1.081	5,887	0.736	84.9
200k S-A	0.366	0.337	1.087	4,818	3.32	369.5
500 k S-A	0.288	0.301	0.957	11,778	0.200	216.3
1.9M S-A	0.309	0.306	1.011	2,898	0.869	99.4
1.3M Polyhedra S-A	0.292	0.301	0.971	7,800	1.533	184.3
1.68M Hexa S-A	0.356	0.319	1.113	3,000	1.600	86.0
1.8M Polyhedra S-A	0.369	0.308	1.199	3,160	0.2÷1.6	20.4
2.5M Polyhedra S-A	0.338	0.307	1.102	20,000	1.533	186.2
13.8M Hexa S-A	0.337	0.459	0.735	62,005	2.113	13.5
23.5M Hexa S-A	0.337	0.270	1.250	10,382	0.716	84.7
500k T k-kl-w	0.273	0.230	1.189	14,514	0.200	122.5
1.9M T k-kl-w	0.417	0.331	1.260	27,575	0.869	140.4
500k k-ω SST Fluent	0.302	0.270	1.119	18,090	0.200	227.2
1.9M k-ω SST Fluent	0.382	0.268	1.424	91,482	0.869	102.7
1.68M k-ω SST Fluent	0.320	0.285	1.122	2,000	0.742	84.83
13.8M k-ω SST Fluent	0.290	0.363	0.799	50,005	2.113	13.5
500k SST CFX	0.354	0.323	1.098	633	0.200	423.7
1.9M SST CFX steady	0.295	0.296	0.997	100	0.869	184.7
1.6M k-ω SST OpenFoam	0.347	0.253	1.371		0.742	47.37
530kRNG k-ε PowerFLOW	0.367	0.543	0.677	62,736	5	269.6
7.69M RNG k-ε PowerFLOW	0.396	0.476	0.832	174,558	1.8	98.56
500k SAS Fluent	0.320	0.307	1.043	11,273	0.2	224.4
1.9M SAS Fluent	0.3662	0.3093	1.184	2,787	0.869	103.6
500k v2f Fluent	0.3405	0.3221	1.057	1,000	0.322	308.4

Table 2. *Simulation results for the Ahmed Body with 12.5⁰ slant angle*

Turbulence model	Mesh size	Ahmed Body Slant 12.5⁰			
		Cd	Avg y+	CPU h	Ds [mm]
LES+WALE	14.5M	0.2283	11.6	584	0.2
RKE	14.5M	0.2246	16.2	624	0.2
DES+rke	14.5M	0.2446	16.1	50	0.2
DES+SST k-ω	14.5M	0.2405	19.1	369	0.2
RSM	14.6M	0.2248	30.4	280	0.2-1.6
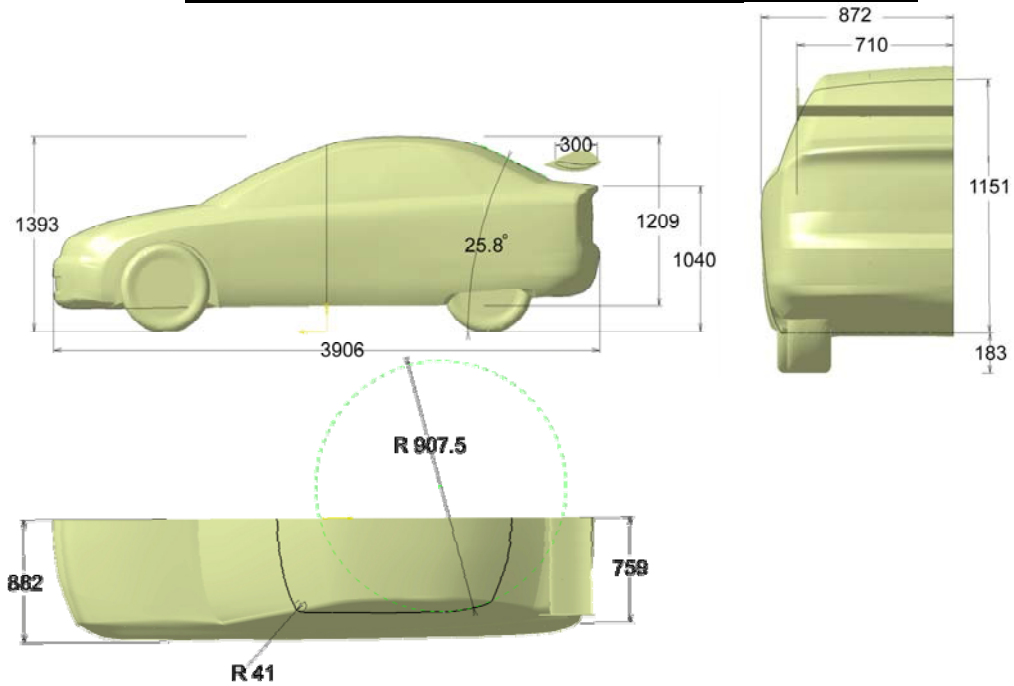
Fig. 2. *Geometry of the simplified car model from [4] and the rear wing (dimensions given in mm)*
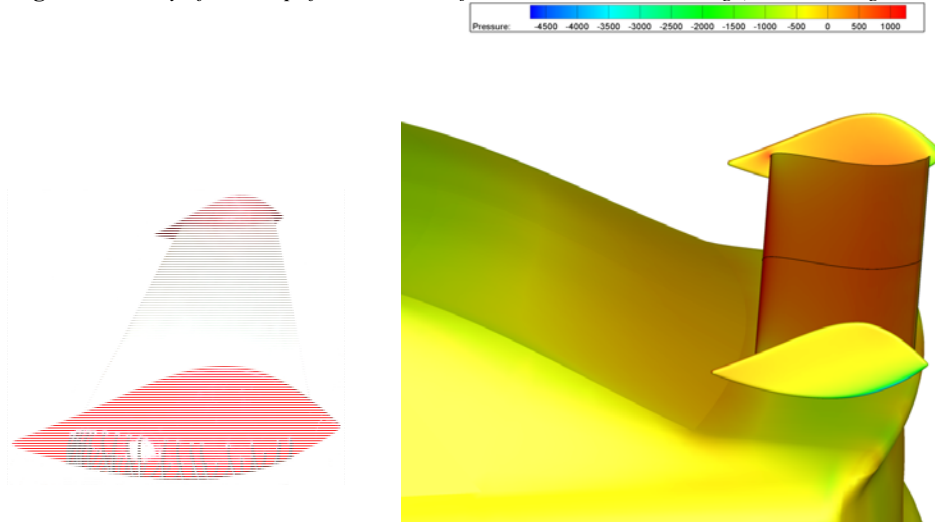
Fig. 3. *The 1ˢᵗ real (left) and the virtual prototype (right) for the rear wing*

Velocity Initialization
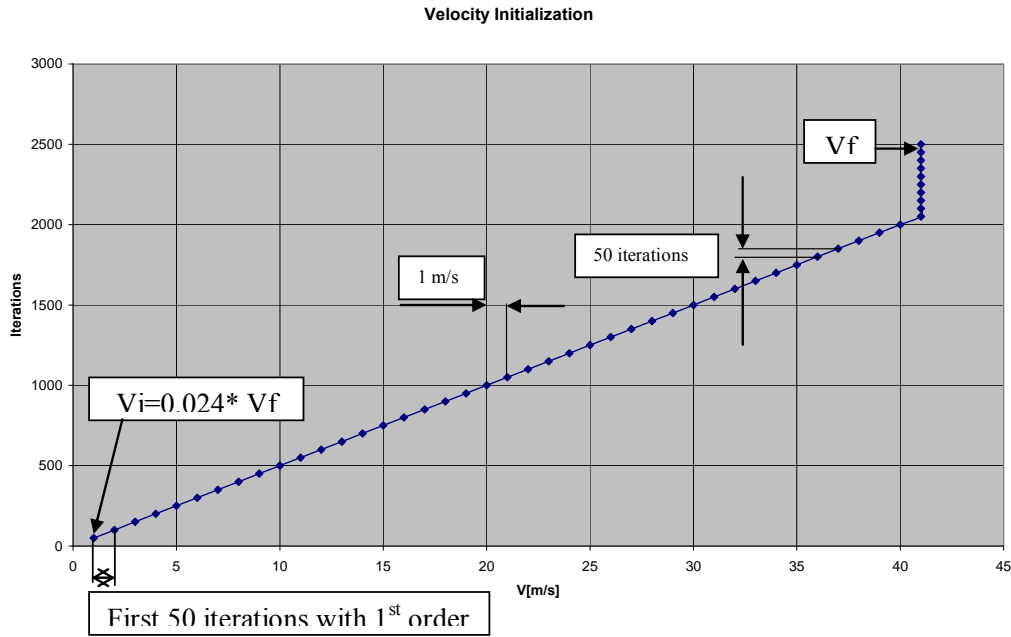
Fig. 4. *The Velocity profile for the intialization*
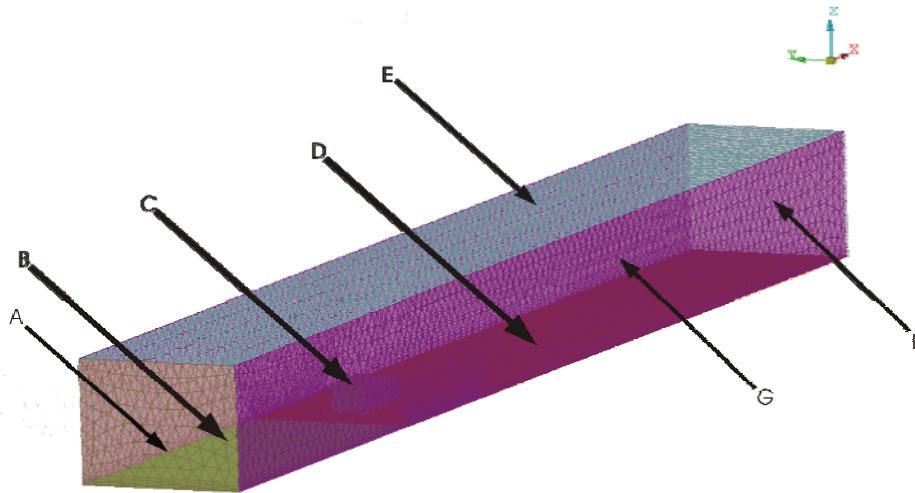
Fig. 5. *Boundary labels for the Ahmed body with 25° slant angle*

Table 3. *Boundary conditions for the Ahmed Body with 25° slant angle*

Boundary	Fluent	CFX	OpenFoam	PowerFLOW
A=inlet	*velocity-inlet*	*inlet*	*inlet*	*inlet velocity*
B=road slip	*symmetry*	*free slip wall*	*slip*	*frictionless wall*
C=Ahmed body	*wall, no slip*	*wall, no slip*	*wall, no slip*	*wall, no slip*
D=road no slip	*wall, no slip*	*wall, no slip*	*wall, no slip*	*wall, no slip*
E=sealing	*symmetry*	*free slip wall*	*slip*	*frictionless wall*
F=outlet	*pressure-outlet*	*outlet*	*inletOutlet*	*outlet: static pressure, free flow direction*
G=side walls	*symmetry*	*free slip wall*	*slip*	*frictionless wall*
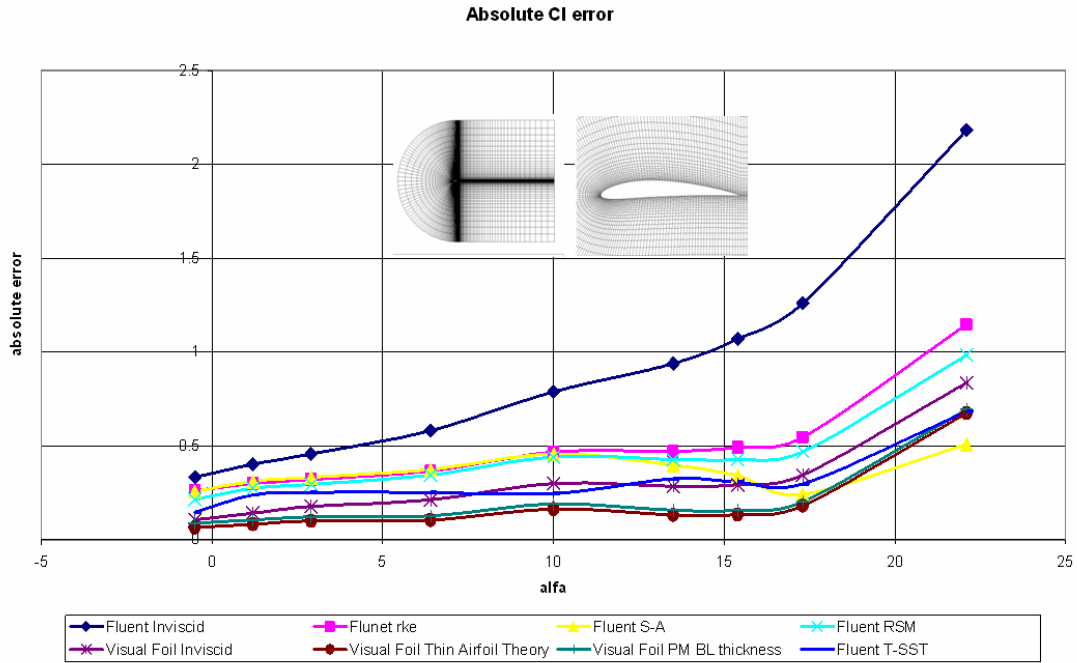
Fig. 6. a. *Comparsion between different numerical experiments and the reference physical one for the CI absolute error of a NACA 4412 airfoil for different angles of attack*
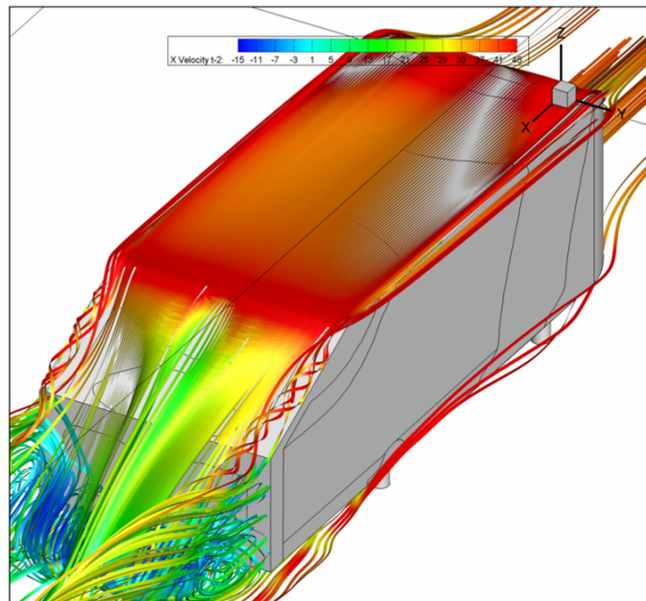
Fig. 6. b. *Streamlines for the 25° slant, 13.8M, k-ω SST Fluent case*
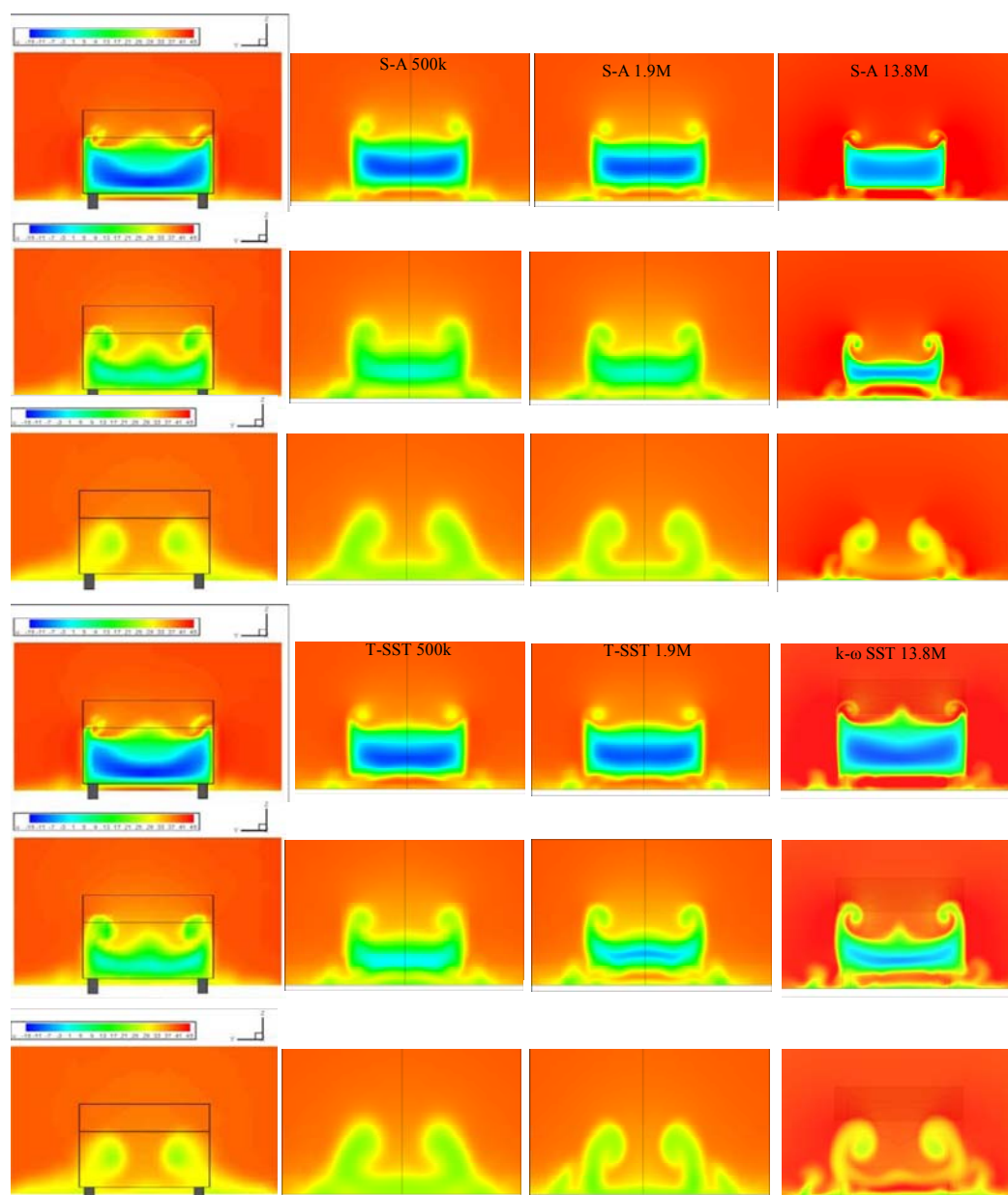
Fig. 7. a. *Streamwise velocity distribution at X=80 mm, 200 mm, 500 mm. Experiment, simulation on coarse, fine grid (left to right) for the "Ahmed body" with 25° slant angle. Fluent turbulence models: S-A, T-SST*
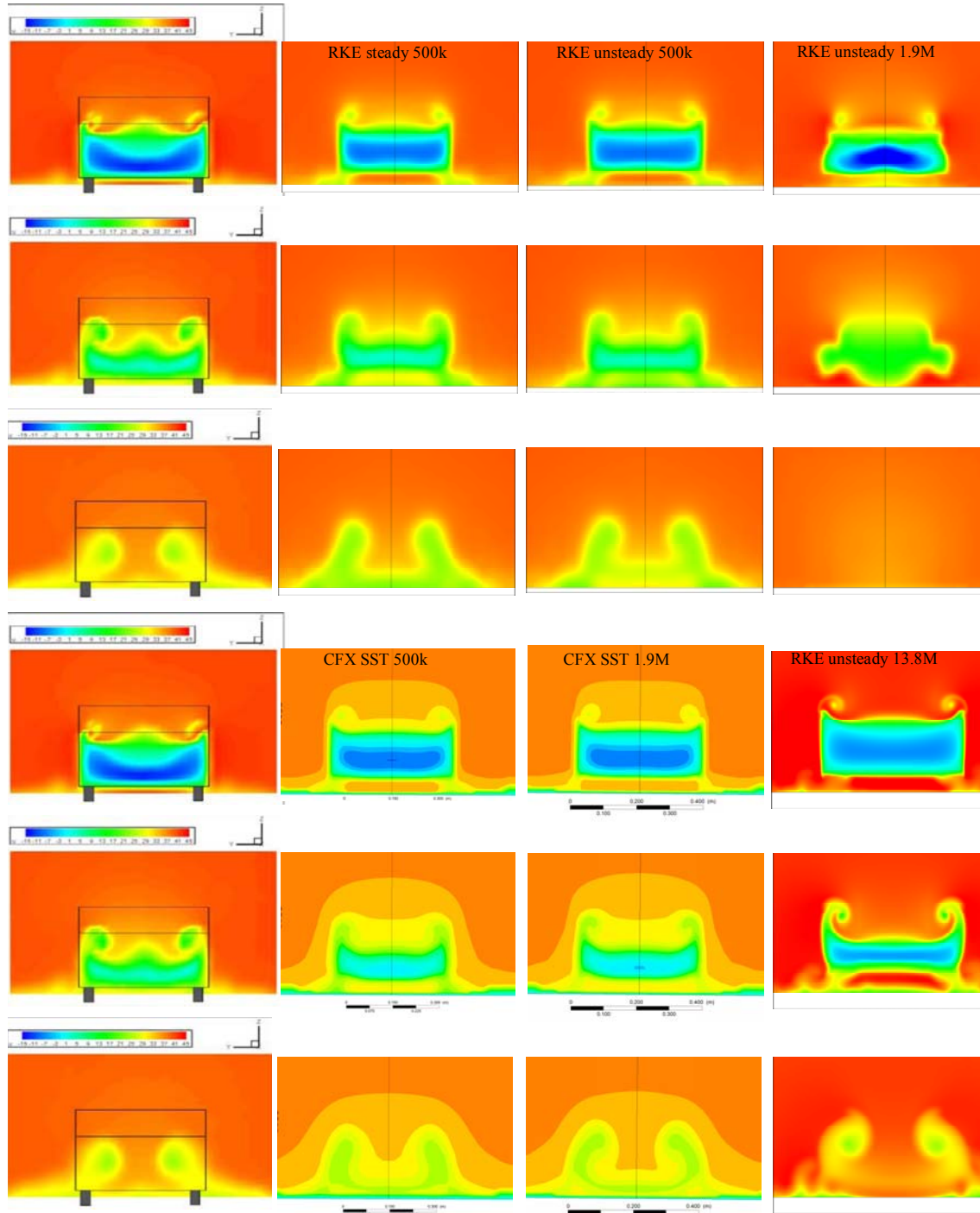
Fig. 7. b. *Streamwise velocity distribution at X=80 mm, 200 mm, 500 mm. Experiment, simulation on coarse, medium and fine grid (left to right) for the "Ahmed body" with 25° slant angle. Fluent turbulence models: RK steady and unsteady and CFX's SST*

Table 4. *Grids for the Ahmed Body*

Mesh size [elements]	Base level [mm]	Surface level [mm]	Volume elements	No. of elm. in the BL	Full or ½ Ahmed Body	Meshing software
200k	160	10	hexas, tetras	0	half	ANSA 13
500k	160	5	hexas, tetras	0	half	HARPOON
530k	160	5	Hexas	2	full	PowerFLOW DISCRETIZER
1.3M	160	5	polyhedras, hexas	0	half	HARPOON
1.68 M	270	5	hexas, tetras, prisms	5	full	ANSA 13
1.79M	160	5	polyhedras, hexas	5	full	ANSA 13
1.9 M	160	2.5	hexas, tetras	2	half	HARPOON
5M	160	2.5	polyhedras, hexas	2	half	HARPOON
7.69 M	28.8	5	Hexas	2	full	PowerFLOW DISCRETIZER
13.8M	80	5-0.625	hexas,tetras	12	full	HARPOON
14.58 M	80	1.25	hexas,tetras	2	full	HARPOON
14.6 M	80	1.25	hexas,tetras	2	full	HARPOON
23.5 M	30	0.93	hexas,tetras	0	full	HARPOON
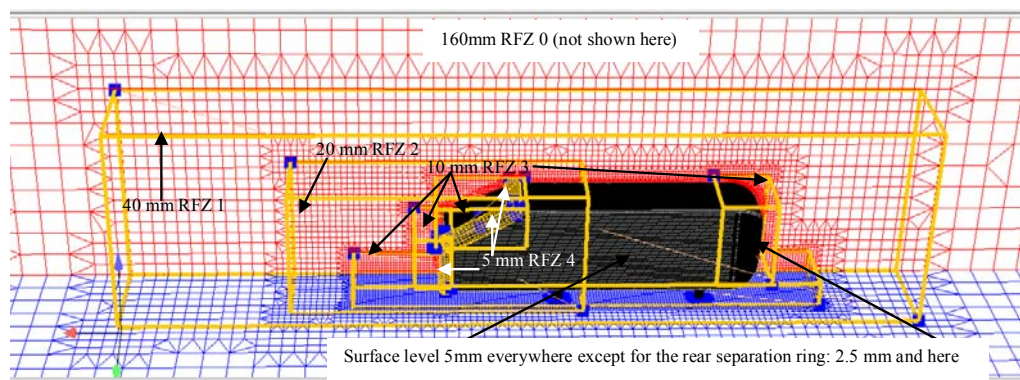
Fig. 8. a. *Coarse grid (500k) for the "Ahmed body" with 25° slant angle*
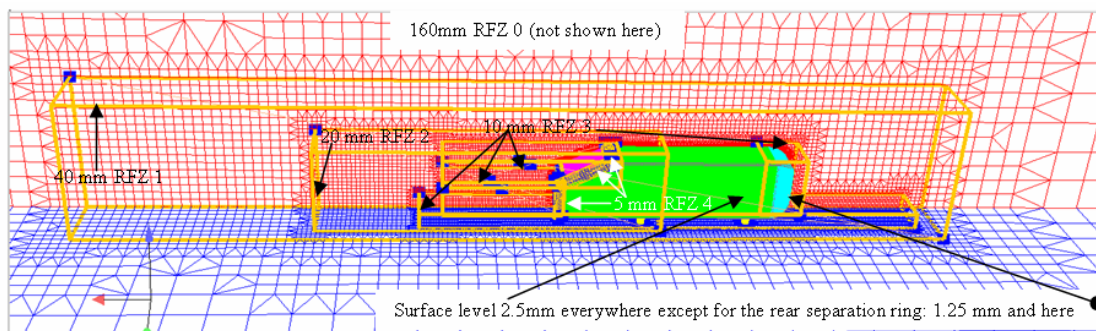
Fig. 8. b. *Medium grid (1.9M) for the "Ahmed body" with 25° slant angle*
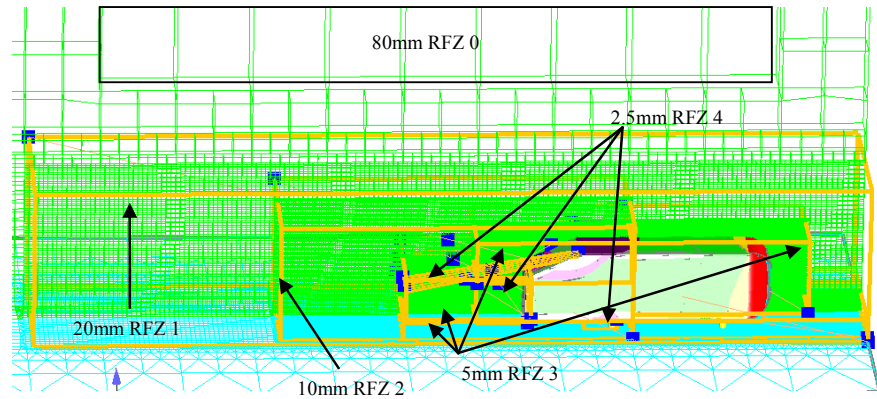
Surface level is adapted (in a previous reference simulation) after the Cp and varies from 5mm to 0.625mm

Fig. 8. c. *Fine grid (13.8M) for the "Ahmed body" with 25° slant angle*
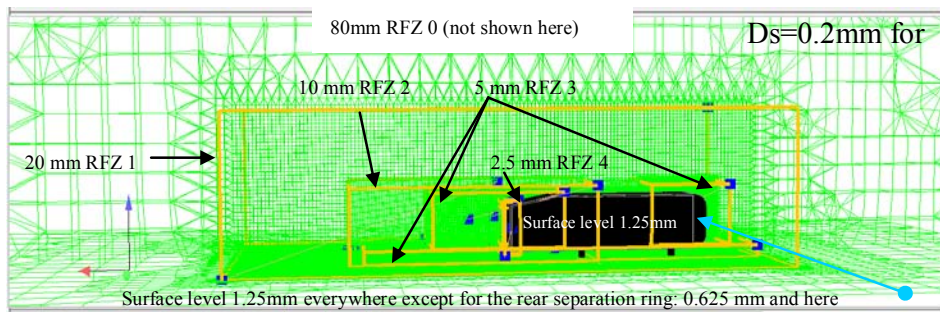
Fig. 8. d. *Fine grid (14.58M) for the "Ahmed body" with 25° slant angle*
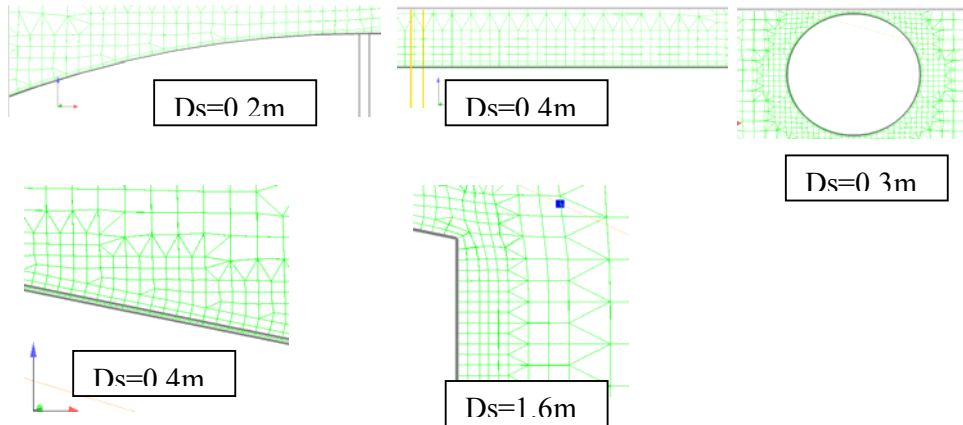
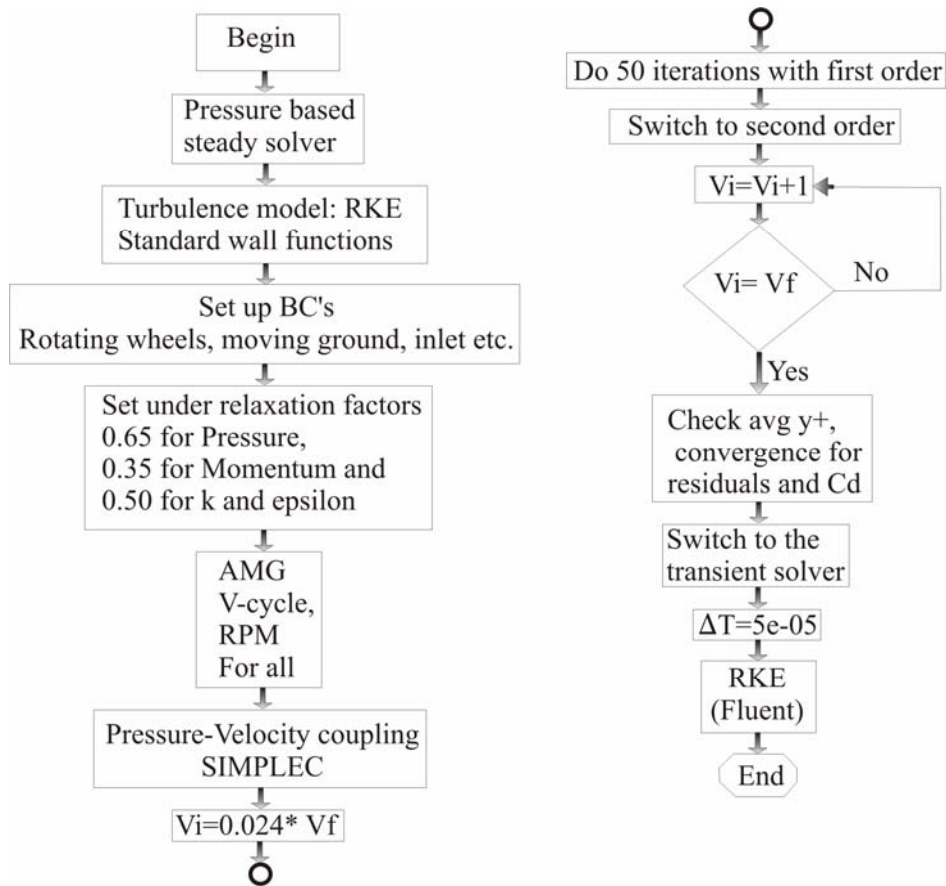**Fig. 8. e.** *Fine grid (14.6M) for the "Ahmed body" with 25° slant angle*

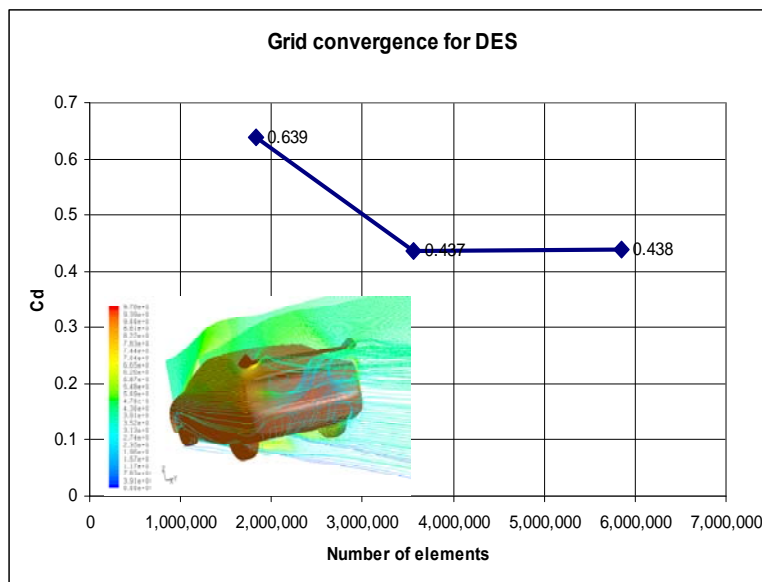**Fig.9.** *Road map for turbulence modeling and transient calculation*

Fig. 10. *Grid convergence for DES and streamlines for the simplified car geometry from [4]*
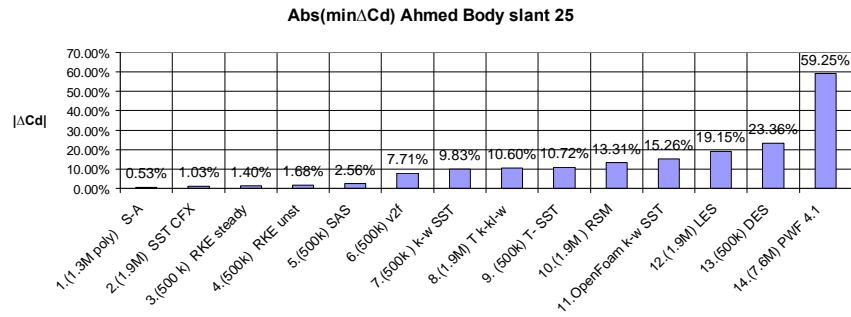
Fig. 11. *Absolute values for minimum Cd for the 25° slant angle*
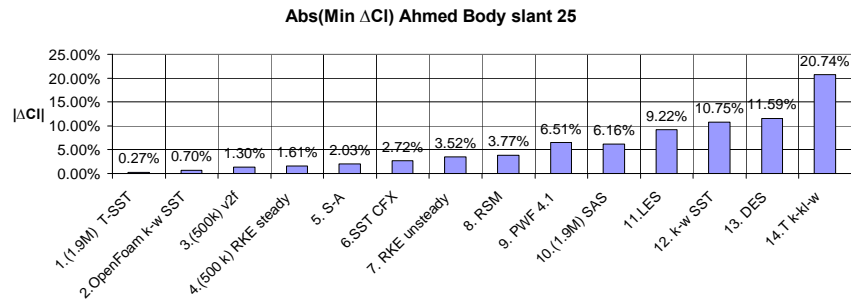
Fig. 12. *Absolute values for minimum C1 for the 25° slant angle*
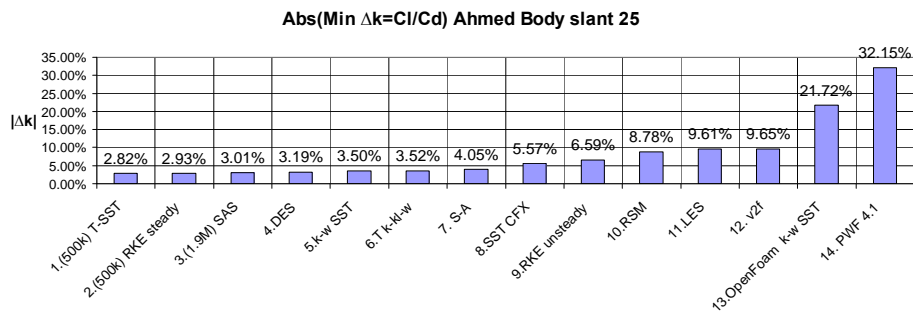
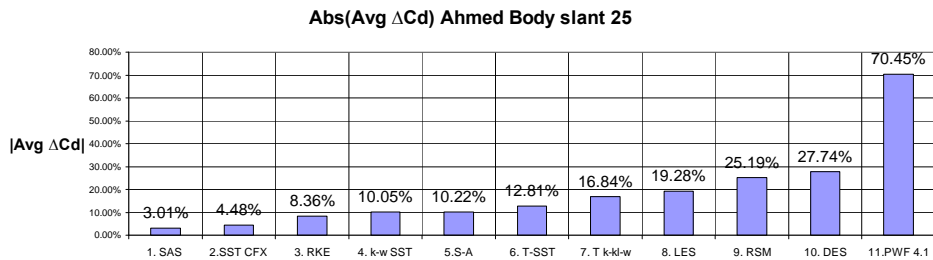**Fig. 13.** *Absolute values for minimum C1/Cd for the 25°slant angle*
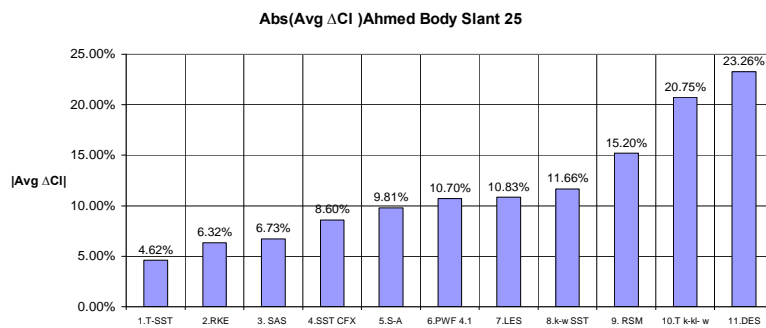

Fig. 14. *Absolute values for 25° slant angle*

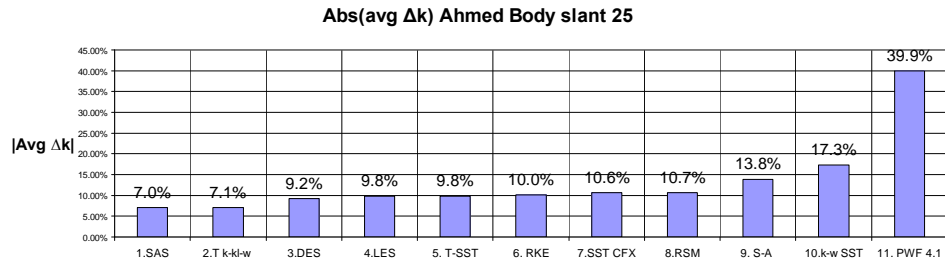**Fig. 15.** *Absolute values for average C1 for the 25° slant angle*

Abs(avg Δk) Ahmed Body slant 25

Fig. 16. *Absolute values for average C1/Cd for the 25° slant angle*

Abs(ΔCd) Ahmed Body slant 12.5
14M Grid
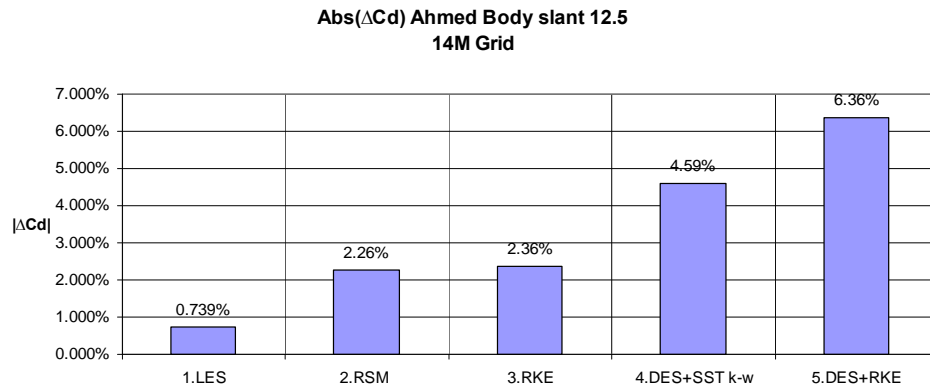
Fig. 17. *Absolute values for minimum C1 for the 25° slant angle*
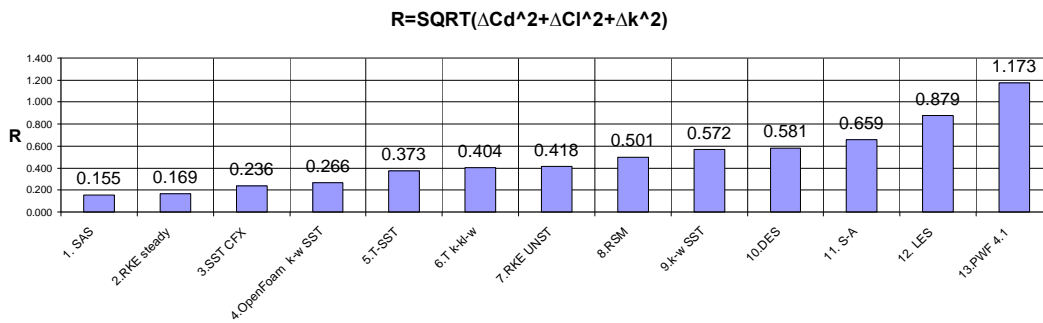
R=SQRT(ΔCd^2+ΔCl^2+Δk^2)

Fig. 18. *Simultaneous drag, lift and aerodynamic efficiency quantitative indicator for all the simulations with the 25° slant angle*

Rezolvarea numerică a unei probleme de aerodinamică pentru un autoturism de curse

—Rezumat—

Utilizarea simulărilor numerice atrage, în prezent, un interes în creştere în optimizarea formelor aerodinamice. Articolul prezintă, în primul rând, rezultatele unui benchmark aprofundat a diferitelor simulări numerice realizate cu Fluent, CFX, OpenFOAM şi PowerFlow pe un profil Ahmed, în scopul de a selecta un model optim şi algoritmul numeric pentru rezolvarea unei probleme de aerodinamica autoturismelor. Descriem, de asemenea, strategiile numerice pentru reducerea timpilor de pregătire, discretizare, simulare si optimizare a modelării numerice a unei probleme de aerodinamica. În al doilea rând, analizăm rezultatele modelării numerice a curgerii în jurul unui profil aerodinamic NACA. Am aplicat strategiile stabilite în prima parte a lucrării în vederea simulării curgerii în jurul unei maşini de curse în trei volume. Rezultatele obținute arată că strategia aleasă calculează cu exactitate forțele de rezistență la înaintare, forța deportantă şi eficiența aerodinamică cu un timp de calcul scăzut.